A Constrained Geostatistical Approach for Efficient Multilevel Aquifer System Characterization

Hayet Chihi[*1], Guislain de Marsily[2], Matthieu Bourges[3], Habib Belayouni[4], Mohamed Sbeaa[1]

[1]Georesources Laboratory, Centre for Water Research and Technologies, University of Carthage, Borj Cedria Ecopark, PO Box 273, Soliman, Tunisia

[2]Sorbonne Universités, UPMC Univ. Paris 06, UMR 7619 METIS, 75005 Paris, France; CNRS, UMR 7619 METIS, 75005 Paris, France; EPHE, UMR 7619 METIS, 75005, Paris, France

[3]Geovariances, 49 bis avenue Franklin Roosevelt, 77215 Avon cedex, France

[4]Department of Geology, Faculty of sciences of Tunis, University of Tunis El Manar, 1068 Tunis, Tunisia

[*1]hayet_chihi@yahoo.fr; [2]gdemarsily@aol.com; [3]bourges@geovariances.com; [4]hbelayouni@yahoo.com

***Abstract*-In this study, the problems of parameter estimation for systems with scarce measurements are examined. In this case, an original geostatistical methodology is applied to generate bathymetric surface models of a faulted aquifer system within the Jeffara Basin in southeastern Tunisia. The modelling workflow is based on i) the spatial analysis of the data configuration and ii) the conceptual stacking pattern. This allows provision of key concepts and geostatistical approaches to be undertaken during geomodelling procedures. In fact, two constraints have been integrated: i) inequality data provided by the end of the boreholes and ii) the faults that compartmentalize the aquifer system. First, kriging with inequality was used for depth estimation of the Turonian reservoir Top. The results are compared with those from classical kriging and evaluated through the estimation quality, the adopted assumptions and the method limitations. Validation analyses show that the model developed with the inequality data leads to a significant gain in mapping accuracy and geological realism. In the second step, the geostatistical approach was used to model the successive bounding surfaces of the aquifer system units. Consequently, the kriging constrained by inequality data could be applied in a variety of hydrogeological parameters interpolations to provide significantly better informative maps that are useful for hydrodynamic modelling.**

Keywords- Geostatistics; Surface Interpolation; Exact Data; Inequality Data; Geological Constraints

I. INTRODUCTION

Arid climate conditions and complex geological settings within aquifer systems are at the origin of uneven spatial distribution of water resources. Innovative methodologies for accurate assessment of water availability and quality are required. This necessitates thorough investigation of subsurface structures in order to build conceptual and numerical models related to the stacking pattern that describes the geometry and the extent of reservoir units, as well as how they are organized and relate to each other.

These models provide efficient means for a complete understanding of the hydraulic connectivity distribution that is needed for hydrodynamic modelling. In this case, one of the main concerns is to estimate the bounding surfaces of aquifer system units in order to build a 3D architectural model. Traditionally, these estimations are performed using classical linear estimation or, better, the geostatistical kriging method. However, sparse data measurements and geological constraints often limit the accuracy of the model.

The quality of the generated 3D architectural model depends on the quantity and quality of available information, the definition of geological hypotheses or constraints about the aquifer system geological setting and the modelling approach.

In this paper, we present an original methodology for modelling the geological interfaces of the Jeffara de Medenine aquifer system (Fig. 1). The workflow integrates the management of data inequalities or constraint intervals as well as geological discontinuities such as faults constraints in order to improve the prediction accuracy using geostatistical tools. Various interpolation procedures are applied and compared, including Common Linear Estimation (CLE), Ordinary Kriging (OK) and Kriging with Inequality constraints (KI). Evaluation of the modelling procedures is undertaken by analyzing spatial accuracy measures such as the kriging variance and geological realism of the modelled surfaces. Furthermore, we discuss the limitations of KI and the developments that were needed to overcome them. The discussed tools and methods are illustrated with reference to two bounding (Turonian and Jurassic) surfaces.

DOI: 10.5963/JWRHE0503002

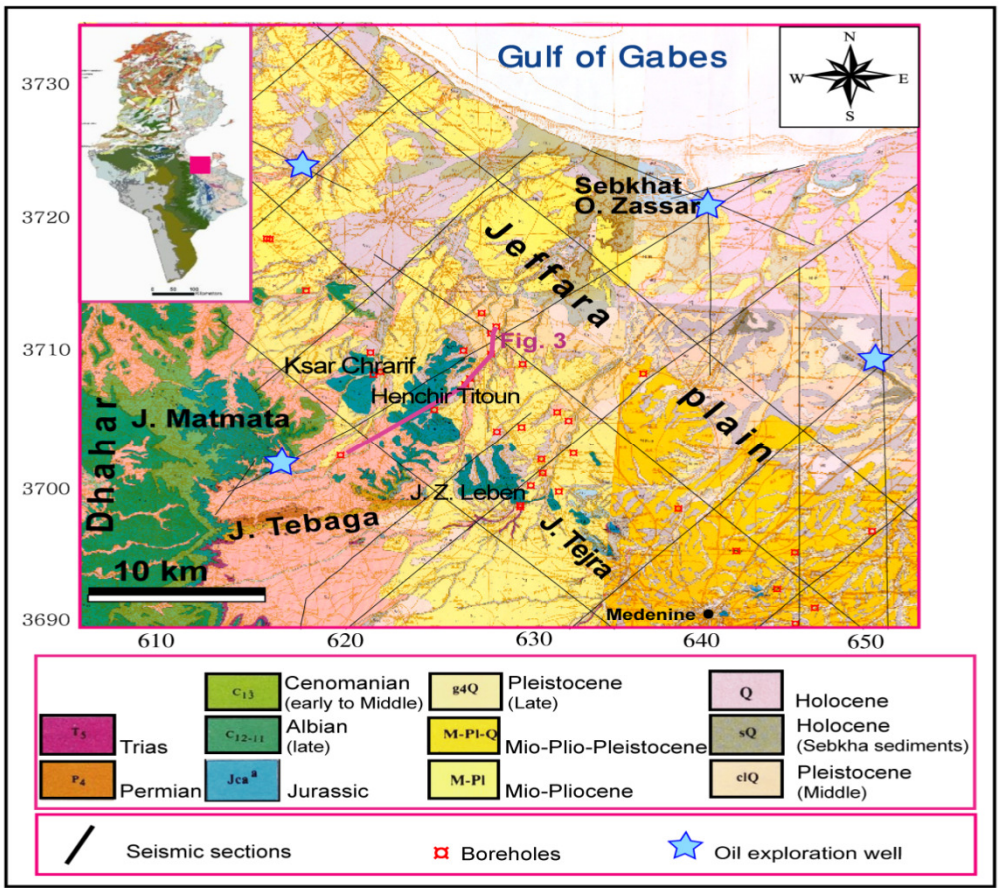

Fig. 1 Study area, geologic setting and data (seismic sections, petroleum wells and boreholes) location

II. GEOLOGY OUTLINES

The "Jeffara de Medenine" multilevel aquifer system lies in the Jeffara basin, situated in southeastern Tunisia (Fig. 1). The most significant water reservoirs are hosted within the Jurassic, Albo-Aptian, Turonian and Senonian series (Fig. 2) [1-4]. The Mio-Plio-Quaternary geological cover lies directly over these aquifer formations by means of an erosional contact [5-6]. The area has been altered by intense and repeated tectonic activity [7-12] that resulted in a complex geological framework.

A thorough stratigraphic and structural framework reconstruction of the study area was accomplished in order to highlight the existing relations between the aquifer system units [4, 13-14].

Sixteen seismic sections and four petroleum exploration wells (Fig. 1) were acquired for a seismic structural study of the area [13]. The locations and lineaments of the faults interpreted from seismic data were drawn on the geological map to build the fault network on a large scale (Fig. 3). 49 boreholes were also used for lithostratigraphic correlation, to construct seventeen geological cross-sections (Fig. 4) and to interpret the small-scale faults [4, 14].

Fig. 5 shows the updated map [4] of the most important normal faults, which strike northwest-southeast and northeast-southwest.

This faulting system splits the study area into horst and graben blocks and engenders a global downtilting with important lateral facies and thickness variations toward the northeast direction.

DOI: 10.5963/JWRHE0503002

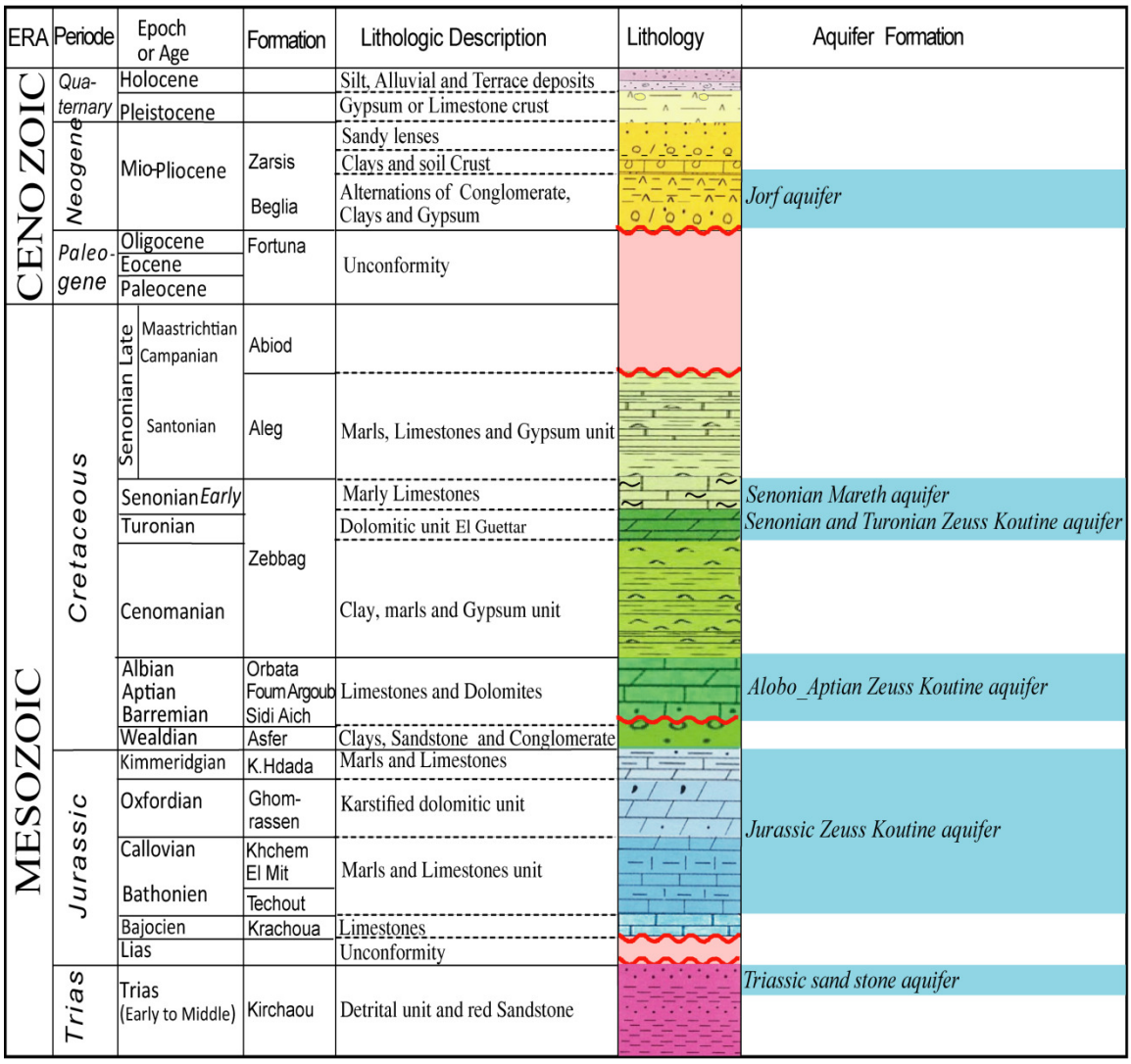

Fig. 2 Stratigraphic section and neighboring formations of the study area [4]

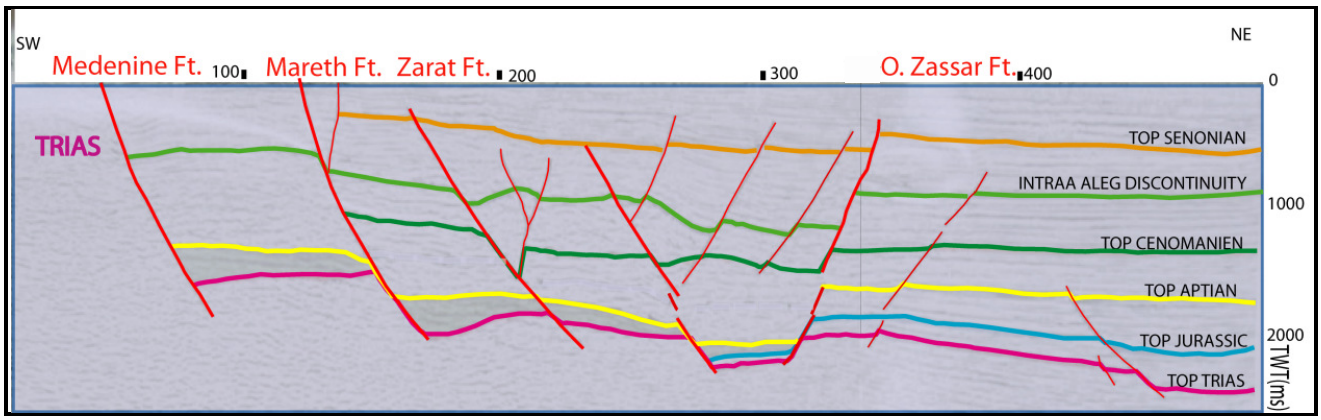

Fig. 3 East-west oriented seismic section through the southeastern part of the study area showing normal faulting

DOI: 10.5963/JWRHE0503002

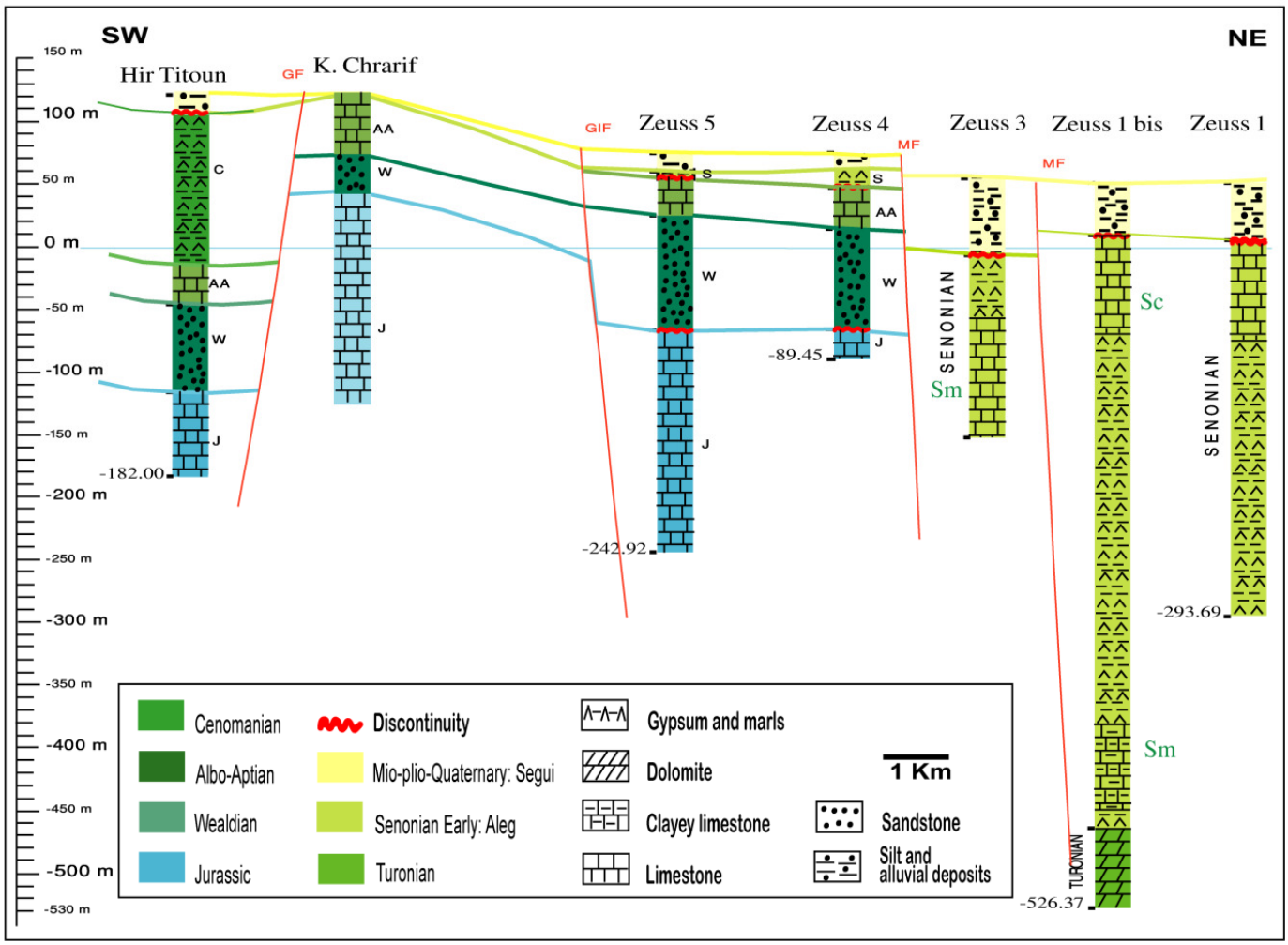

Fig. 4 Geological cross-section along the southwest-northeast direction, showing traces of major faults and lateral facies and thickness variations within the study area [4] (see Fig. 1 for location)

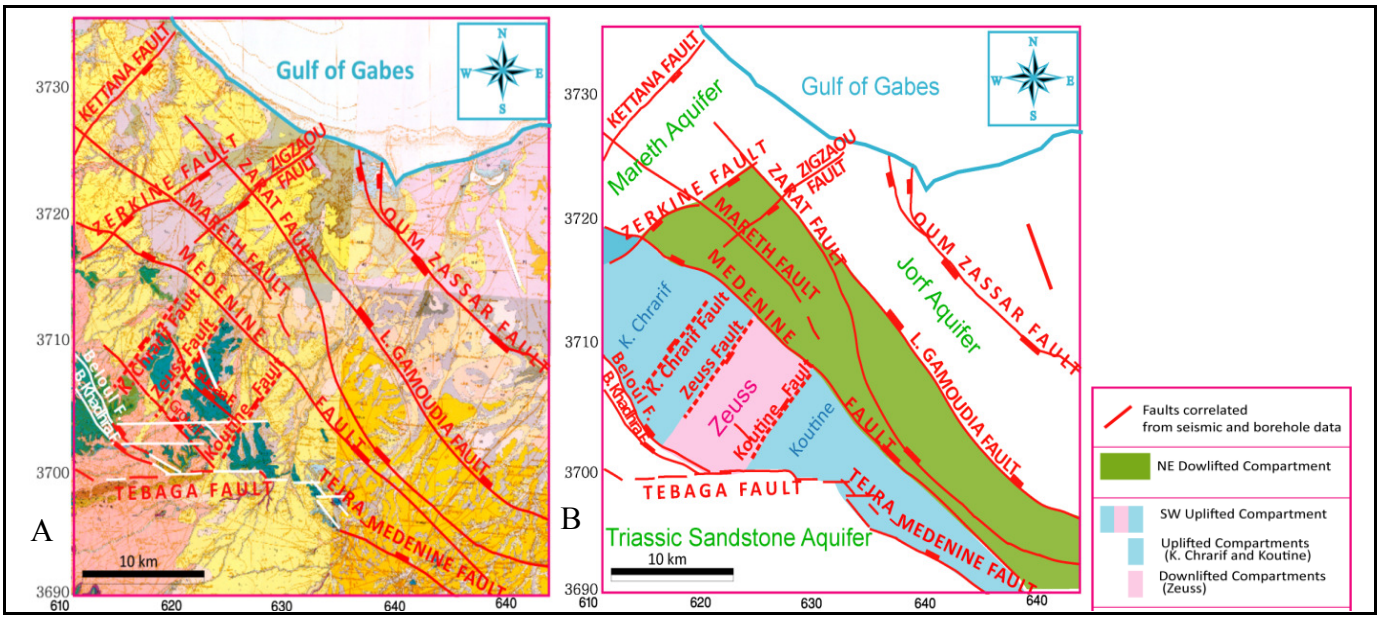

Fig. 5 Major normal faults mapped from seismic and geological data (A) and main structural compartments (B) [4, modified]

Accordingly, the study area is characterized by two geological compartments that are separated by the Medenine fault (Figs. 3, 4 and 5). The southwest uplifted compartment contains Jurassic and Lower Cretaceous formations composed mainly of carbonate and sandy lithologies (Fig. 4). The northeast downshifted compartment includes the Upper Cretaceous formations

DOI: 10.5963/JWRHE0503002

composed mainly of carbonate, clay and gypsum (Fig. 4). A thick alluvial formation of the Mio-Plio-Quaternary age covers the major part of the study area.

The Koutine sub-compartment (Fig. 5B) is an uplifted compartment and consists mainly of Jurassic carbonates. The locally encountered Albo-Aptian sediments are composed of dolomite and limestone.

The Zeuss sub-compartment (Fig. 5B) is a collapsed compartment. It includes a thick sedimentary sequence composed of carbonate and sandy formations of the Jurassic, Wealdian, Turonian and Albo-Aptian periods. This sedimentary sequence is covered by thick Mio-Plio-Quaternary sediments.

The Ksar Chrarif sub-compartment (Fig. 5B) is an uplifted compartment that consists mainly of carbonate and sandy formations of the Jurassic, Wealdian and Albo-Aptian intervals. Cenomanian sediments also are encountered locally.

III. ARCHITECTURAL MODELLING

The framework for the aquifer system is assumed to consist of several bounding faulted surfaces, as illustrated in Figs. 3 and 4. An architectural model of the aquifer system was created by modelling these geological interfaces independently, such as honoring available borehole data, using the geostatistical software ISATIS [15]. In the following, we detail the modelling procedures and results for the four geological interfaces bounding the main units. The mapping is accomplished by interpolating topographic elevation Z variables (measured in meters) and noted as "Jurassic Horizon", "Cenomanian Horizon", "Turonian Horizon" and the "Senonian Horizon".

We implement an original geostatistical approach to constrain prediction of the depth variable at unsampled locations, while taking into account simultaneously:

1) the random spatial distribution of the data, and

2) the fault geometric parameters that contribute to split the surfaces to be estimated into areas constrained by unequal data density.

A first attempt was published in [14], which presents the modelling results for just one surface of the aquifer system. In the present paper, we outline, while presenting the improvements made to the methodology, the modelling steps of the bounding surfaces of the aquifer system units.

Under these circumstances and to emphasize the efficiency of this approach, three main methods have been applied with comparative results. The first method consists of a common linear estimation. The second method is based on the primal form of kriging, but constrained by fault discontinuity parameters. The third method is based on Kriging constrained by the inequality data.

As a first step and to compare the efficiency of the 3 methods (classical linear estimation (CLE), ordinary kriging (OK) and kriging with inequality (KI)), we choose to estimate the Turonian Horizon, for the reason that we have both exact and inequality data within the northeast downlifted compartment. In the second step, we present different trials to estimate the Jurassic Horizon. We also discuss the limitations and improvements of the kriging with inequality method. In the third step, we briefly present the estimation results of the Cenoamnian and Senonian Horizons. Finally, we outline a discussion of the modelling results to emphasize the efficiency of the elaborated geostatistical approach in reproducing the geological reality of the Jeffara de Medenine aquifer system.

A. Exploratory Data Analysis

The surfaces' modelling was carried out using information from seismic cross-sections, petroleum wells and boreholes (Fig. 1). Seismic and petroleum well data were examined and interpreted in previous works [13] on the study area to map the prominent fault network.

The data from the water wells were collected, organized and recorded in a georeferenced database with the seismic data and the petroleum wells. The log descriptions were homogenized, reinterpreted, codified and assigned to a formation or group of formations based on available data including the geological map. For the geostatistical studies, the database was constructed by describing different layers of information: the borehole identifier (borehole name, X and Y coordinates, total depth, etc.), geological formation (tops, lithology description, lithostratigraphic classification, age, petrophysical properties, etc.) and faults (name, X and Y location of each vertex).

B. Variographic Analysis

The basic tool for spatial correlation analysis is the experimental variogram function [16-19], which characterizes the spatial structure of the regionalized variable $Z(x)$:

$\gamma(h) = \frac{1}{2}Var[Z(x) - Z(x+h)]$, where h is the lag distance between sample pairs $(Z(x), Z(x+h))$.

DOI: 10.5963/JWRHE0503002

To be used in the kriging interpolations, the experimental variogram requires fitting by a theoretical definite positive function, taking into account the context of the local and regional geology and the number and the spatial distribution of the available data [13, 4, 19-24]. The theoretical model of the spatial variability is then used to estimate the random variables' "depth" ("Jurassic Horizon", "Cenomanian Horizon", "Turonian Horizon" and the "Senonian Horizon") at unsampled locations.

The experimental variograms of the different "depth" variables have been calculated in two main geographical directions that cross the two main structural features (i.e. normal faults striking northwest-southeast and northeast-southwest). The provided data are sparse and sampled on an irregular grid (Figs. 1 and 8); thus, it was difficult to choose the parameters required for calculating the experimental variograms. Many attempts were made to select the best values of the lag distance, tolerance on distance, tolerance on angle direction and maximum distance limit, which are required to identify a reliable spatial correlation function [13, 25-27]. Fig. 6 shows the distinctive shapes of the directional, experimental and theoretical variograms. The variograms are generally characterized by very large variability because of the structural faulting features. The experimental variograms construction is based mainly on pairs of depth observations located on either side of the faults.

The directional variograms of the Senonian and Turonian horizons clearly display anisotropic behavior with a higher variability along the northeast-southwest direction.

The "Turonian Horizon" variable shows an anisotropic behavior in the directional variograms. We observe *(i*) a stationary structure evidenced along the northwest-southeast direction, describing the local depth variability, inside the structural compartment, and *(ii)* a non-stationary structure confirmed along the northeast-southwest direction, reflecting the depth increase in accordance with the area downtilting towards the northeast direction.

The directional variograms of the Senonian Horizon exhibit, in addition to the stationary component that describes the depth variability at a local scale in the northwest-southeast direction, a more prominent drift structure is clearly expressed along both the northeast-southwest and northwest-southeast directions. These drift structures reveal a downtilting of the Senonian Horizon that is more important in the northeast direction.

The directional variograms of the Cenomanian horizon indicate stationary structures with higher variability along the northeast-southwest direction.

The directional variograms of the Jurassic horizon display isotropic stationary behavior. We presume that the drift structure may exist, but is not expressed by the variograms of the Jurassic and the Cenomanian horizons. This is explained by the fact that the drift structure is revealed by the variogram pairs that are calculated from points located on both sides of the Medenine Fault (Fig. 5). Within the northeast compartment, we only have inequality data (Figs. 13 and 14A), which are not considered in the experimental variogram calculation, as only the exact data are taken into consideration.

Taking account of *(i)* these explanations on the spatial variability behavior within the different horizons and *(ii)* the restricted location of the neighborhood as it is explained in the following section, we assume that the theoretical model must be estimated from experimental variogram values at only small and medium lag distances. Consequently, the depth interpolation is based on only the stationary behavior.

Table 1 summarizes the different model parameters (the range *a* and the sill *C*) obtained for each depth variable. The estimated model for the "Senonian Horizon" variable implies two nested anisotropic stationary functions. Anisotropic stationary models fit the Turonian and the Cenomanian variograms.

The "Jurassic Horizon" variable exhibits isotropic behavior, as shown by the directional variograms. Thus, the experimental mean variogram was calculated (Fig. 7) and fitted with a stationary spherical model.

TABLE 1 THEORETICAL MODELS OF DEPTH VARIABLES FOR EACH SURFACE

Variables	Structure	Range (m)		Sill (m^2)	Equation
		N120	N30		
Senonian Horizon	Spherical	1600	4800	500	$\gamma(h) = 500$ spherical $(1600_{N120};4800_{N30})$ + 44000 Gaussian $(65000_{N120};38000_{N30})$
	Gaussian	65000	38000	44000	
Turonian Horizon	Spherical	10000	5000	2000	$\gamma(h) = 2000$ spherical$(10000_{N120};5000_{N30})$
Cenomanian Horizon	Gaussian	3195	5836	2097	$\gamma(h) = 2097$ Gaussian$(3195_{N120};5836_{N30})$
Jurassic Horizon	Spherical	12000	12000	6500	$\gamma(h) = 6500$ spherical(12000)

DOI: 10.5963/JWRHE0503002

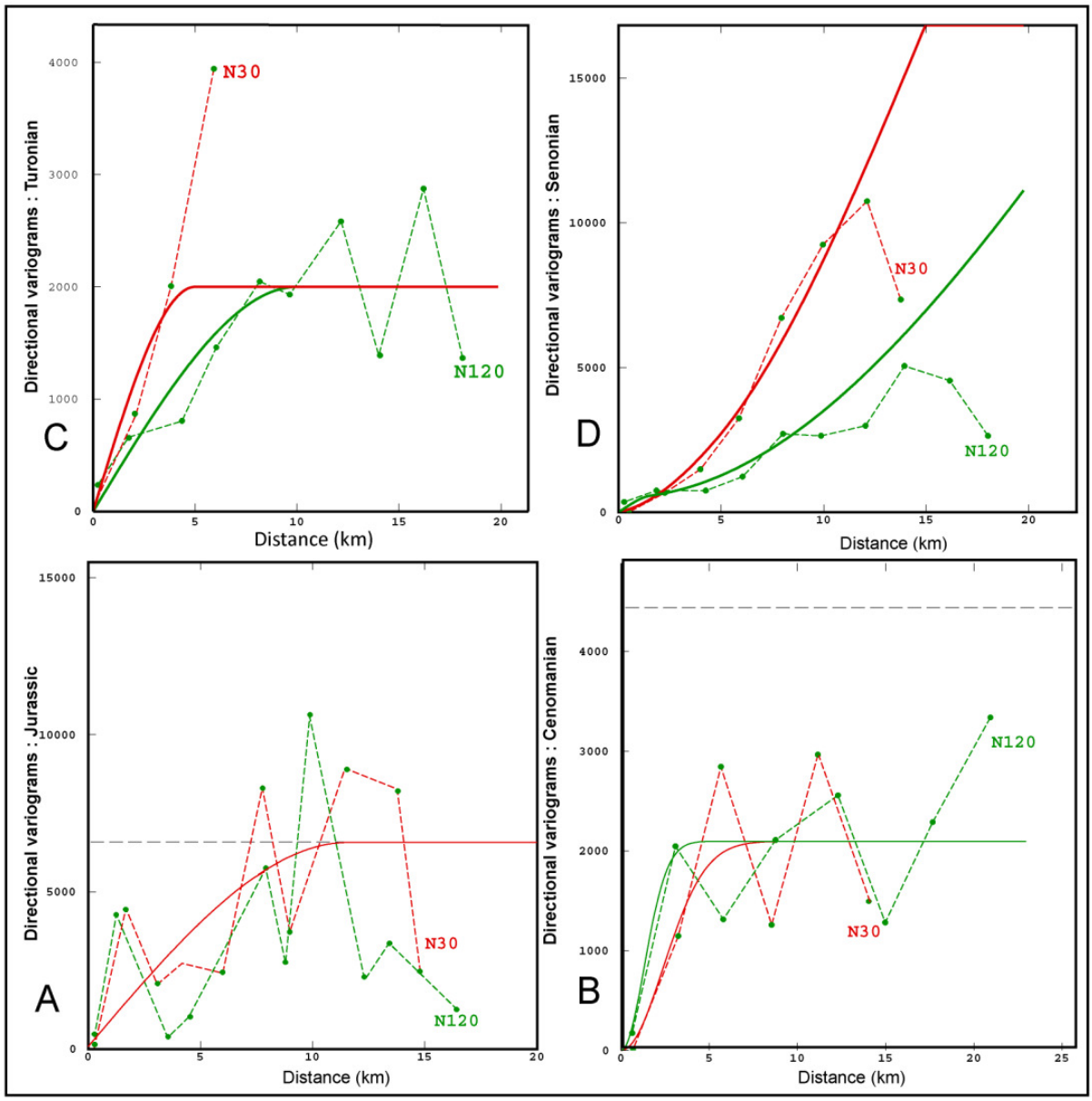

Fig. 6 Directional experimental (- -) and theoretical (——) variograms of the Jurassic (A), Cenoamnian (B), Turonian (C) and Senonian (D) Horizon

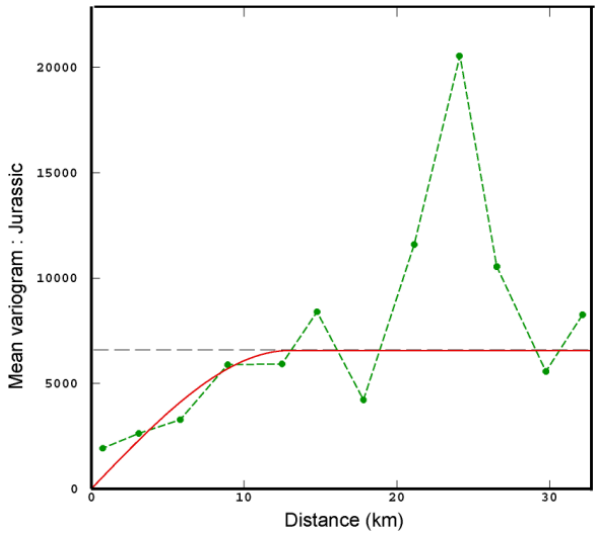

Fig.7 Mean experimental (- -) and theoretical (——) variograms of the Jurassic horizon

DOI: 10.5963/JWRHE0503002

C. Neighborhood

The neighborhood search defines the sampled points used for estimation of values at unsampled locations. In our case study, the estimation procedures, involving OK and KI, were performed taking into account the faulting. This implies that the studied area has to be divided into domains wherein the local variability is respected. Nevertheless, this would lead us to pay more attention to the search neighborhood at compartments with few samples to ensure the most accurate predictions there.

Fig. 8 illustrates that for each target point located in a given domain bordered between faults (i.e, the blue shaded compartment), the kriging neighborhood includes only observations located within this compartment [13, 21-22].

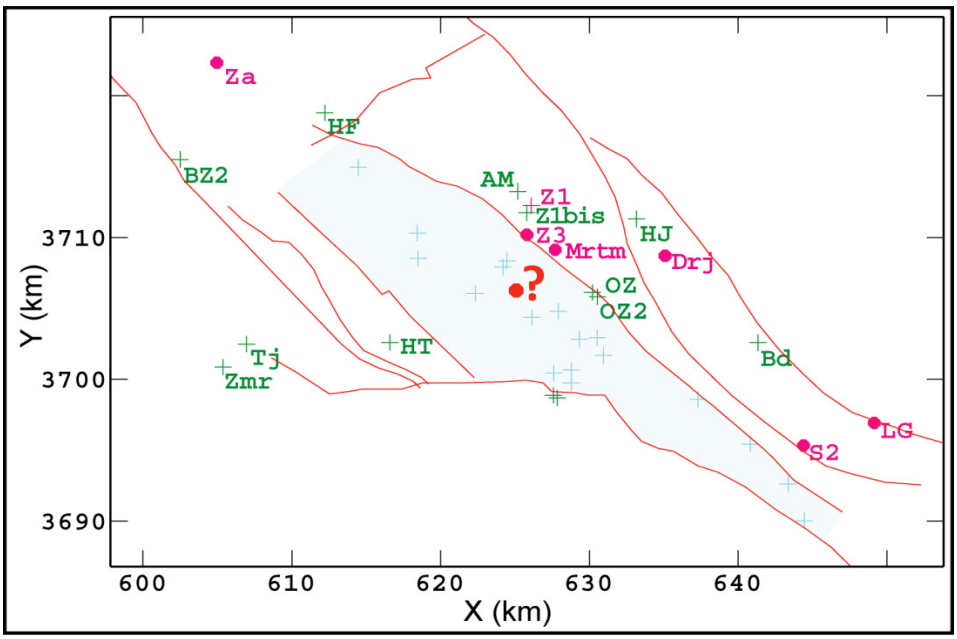

Fig. 8 Implementation of the neighborhood. Only the observations located in the blue structural compartment are used for kriging of any target point in the compartment.
(+: exact data, •: inequality data, —: faults)

D. Surface Estimation

In the following sections, the kriging with inequality prediction [14] is reviewed (Fig. 9) from the perspective of an optimization problem and compared with the OK subject to discontinuity constraints. The latter is compared with the classical linear estimation to emphasize the efficiency of the elaborated geostatistical approach in reproducing the geological reality.

1) Classical Linear Estimation

The depth variable "Turonian Horizon" was first estimated using the classical linear estimation method, based on exact data $Z(x_\alpha) = z_\alpha,\ \alpha = 1, \dots, n$, and a linear regression estimator $Z^*(x)$, which is defined as: $Z^*(x) = \sum_{\alpha=1}^{n} \lambda_\alpha Z(x_\alpha)$. The estimation of the "Turonian Horizon" provides a depth map (Fig. 10) that has a smooth appearance. Therefore, it reflects only the overall downtilting to the northeast direction, but it does not capture the detailed structures. The CLE is inappropriate to closely delineate the local variability. Consequently, it does not reproduce the geological reality. It is also important to note that this method does not provide for each estimated value, the corresponding kriging variance which measures the quality of the estimation. However, this method is still used in hydrogeological parameter estimation.

2) Ordinary Kriging

Ordinary kriging is a powerful linear estimator that is the most common variant of kriging. This method estimates an unsampled value, of the target depth variable of a geologic interface, as: $Z^*(x) = \sum_{\alpha=1}^{n} \lambda_\alpha Z(x_\alpha)$, from n observations $\{Z(x_\alpha), \alpha = 1, \dots, \mathrm{n}\}$,defined as the neighborhood.

The weights λ_α, which are associated with the sampling points, are chosen in a way that reduces the variance of the estimation error $\sigma_k^2 = Var[Z^*(x) - Z(x)]$ while honoring the unbiasedness condition.

The depth variable "Turonian Horizon" estimation was conducted using OK for the given input data set including only exact data and taking into account *(i)* the random spatial distribution of values and *(ii)* the geometric fault characteristics that split the surfaces to be estimated into areas unequally sampled. These constraints are the source of major difficulties that we pay particular attention to, as they could be the origin of uncertainty. Geostatistical methods allow the assessment of the uncertainty on each unsampled value and, thus, create a map of the kriging errors, which may help to choose the appropriate kriging method in order to optimize depth prediction within uneven sampled compartments.

DOI: 10.5963/JWRHE0503002

The kriged map of the upper bounding surface of the Turonian reservoir is displayed in Fig. 11A. As can be seen in the central compartment (C), with higher data density, the OK estimations are accurate enough. This is attested by the low values of the kriging variance displayed in Fig. 11B. However, in compartments (A) and (B), located in the northeast side of the Medenine fault, there are some inconsistencies. This could be explained by the neighborhood design and, more precisely, the observations that have to be restricted inside the considered compartment. Moreover, the information deduced from boreholes that do not reach the horizon to be estimated are not employed during estimation. The neighborhood information are therefore limited, and this generates higher values of the kriging variance.

3) Kriging with Inequality Constraints

Kriging with an inequality constraint allows for use of the information deduced from boreholes that do not reach the geological interface to be employed in the estimation procedures and thus to improve the "depth" variable estimation.

In fact, as illustrated in Fig. 9(1), KI involves the prediction of the depth variable at unsampled locations, including (i) exact values: $Z(x_\alpha) = z_\alpha,\ \alpha = 1, \dots, m$, (for example, $\boldsymbol{Z(x)_{Drouj} = -392\ m}$), and (ii) "inequality data": $Z(x_\alpha) \in A_\alpha = [a_\alpha; -\infty[$, $\alpha = m+1, \dots, n$, (for example, $\boldsymbol{Z(x)_{H.\ Jdidi} \leq -932\ m}$) (Fig. 9(1)).

The KI method presented in this paper is a two-step procedure [14, 22, 28-29]: first, inequality data are transformed into exact data, and then these transformed data are added to the original data set to predict the "depth" variable using OK (Fig. 9).

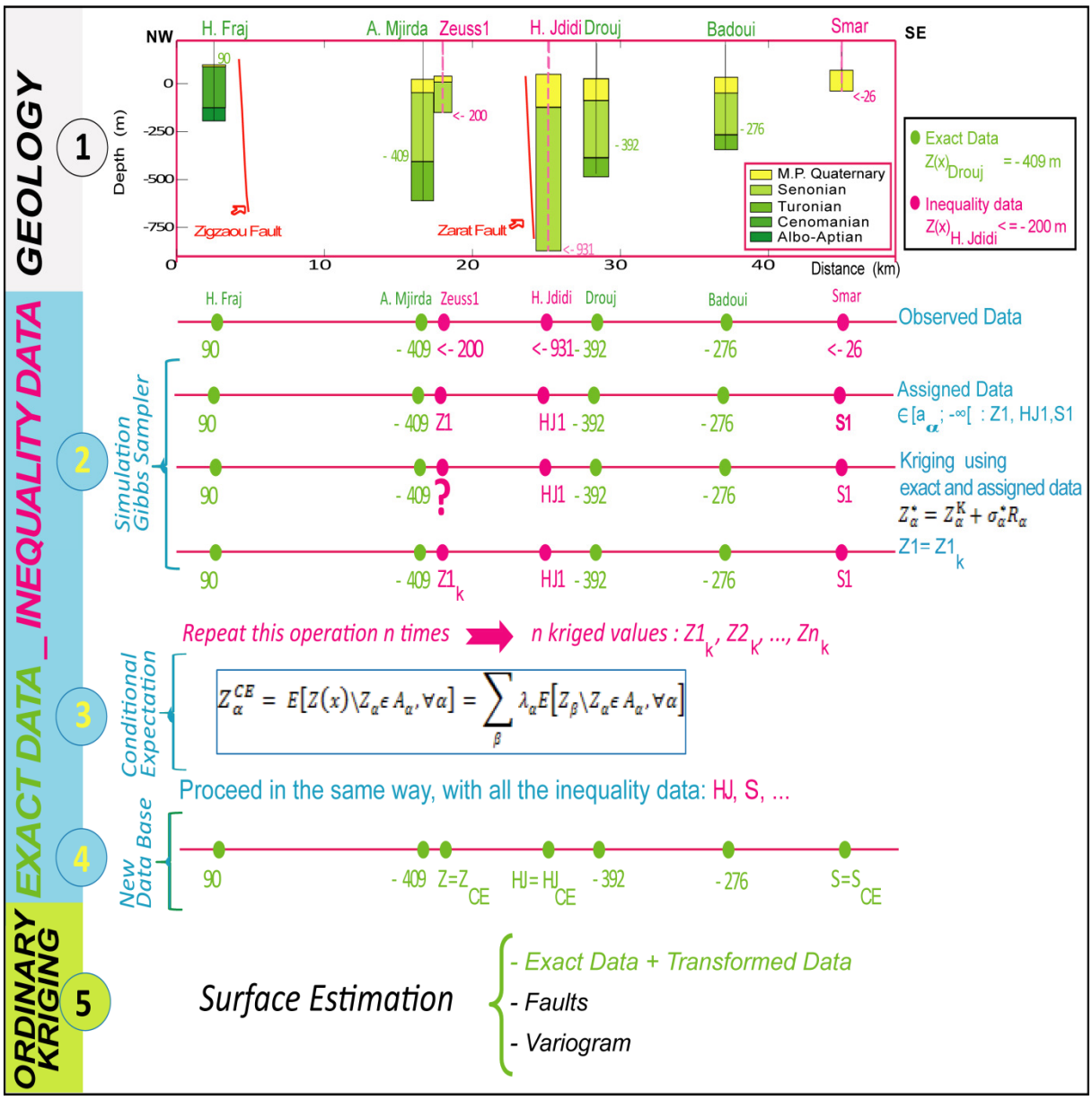

Fig. 9 Detailed workflow of the kriging with inequality method and inequality data transformation using "Gibbs sampler" simulation

Inequality data are converted into exact data by calculating the conditional expectation of the variable at each position x_α of the inequality data Z_α^{CE} (Fig. 9). Expectation is computed using the Gibbs Sampler [22, 28-29] technique. For each

DOI: 10.5963/JWRHE0503002

inequality, several possible conditional simulations are generated based on the spatial variability model and taking into consideration all (exact and inequality) measurements. The simulation realizations are finally averaged at each inequality position x_α. These mean values constitute an estimation of the conditional expectation and are added to the initial data as new exact data.

To simulate $Z_\alpha^{CE}, \propto = m+1, \ldots, n$ conditionaly $Z_\beta = z_\beta$, $1 \le \beta \le m$ and on $Z_\beta \epsilon A_\beta$, $m+1 \le \beta \le n$ including $\beta = \propto$, the following iteration is implemented :

(1) Assign a random value $z_\propto$ within $A_\propto = [a_\propto; -\infty[$ for each site $x_\alpha, \propto = m+1, \ldots, n$.

(2) Select an index α_0 at random in the set of inequality data $\{\propto = m+1, \ldots, n\}$.

(3) Ignore the value at this site and estimate it by kriging from the current values z_β at all other sites; also, compute the corresponding kriging variance $\sigma_{\alpha 0}^{*2}$.

(4) Replace the value at this site by the kriged value plus a simulation of the error, conditionally on the inequality data at $x_{\propto 0}$: the new $z_{\propto 0} = Z_{\alpha 0}^{K} + \sigma_{\alpha 0}^{*} U$, where U is a random normal random variable chosen so that $z_{\propto 0}$ honors the inequality.

(5) Go back to 2, and loop many times.

(6) Calculate the conditional expectation at this site by averaging the set of simulations $z_{\alpha,}$ $(\alpha = m+1, \ldots, n)$. The conditional expectation Z_α^{CE} is in fact the most probable value of the variable at the inequality data locations.

$$Z_\alpha^{CE} = E[Z(x) \backslash Z_\alpha \epsilon A_\alpha, \forall \alpha] = \sum_\beta \lambda_\alpha E[Z_\beta \backslash Z_\alpha \epsilon A_\alpha, \forall \alpha] \quad [22]$$

Consequently, the extended data set including initial exact data and transformed inequalities are used for kriging the geological interfaces. This enables an increase in the neighborhood information within each compartment and, therefore, a decrease in uncertainty.

Practically, the constrained kriging method makes it possible to involve inequalities observed on boreholes that do not intercept the Turonian horizon and to enhance the surface calculation (Fig. 12A). It can be seen in Fig. 12B that the depth estimation is successful along all the different domains of the study area. In the north-eastern compartments A and B, where there are few available samples, the accuracy of the estimates is improved since inequalities are currently efficiently utilized in the depth estimation. This leads to a decrease in the estimation error variance within the two compartments and, especially, nearby the inequalities.

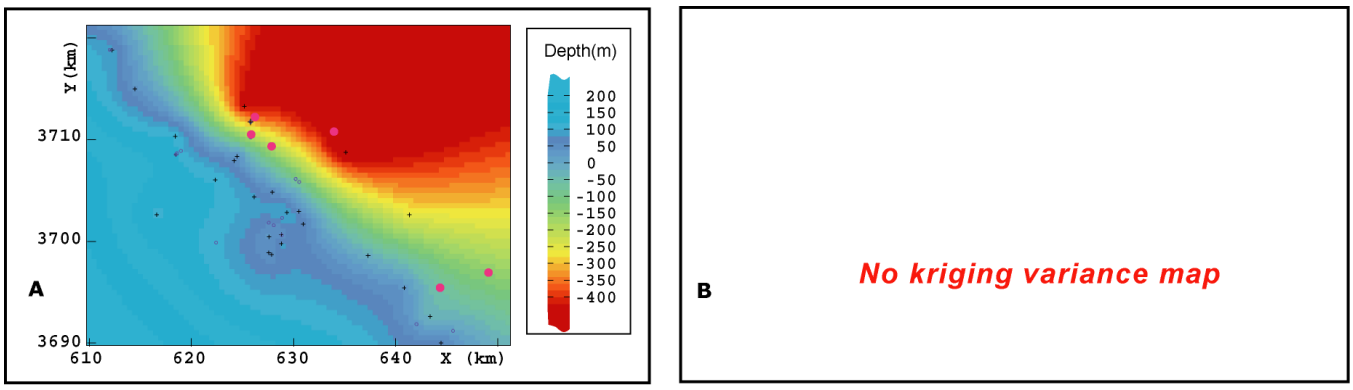

Fig. 10 A: Upper surface of the Turonian reservoir estimated by CLE. (+: exact data, •: inequality data). B: No kriging variance map is provided

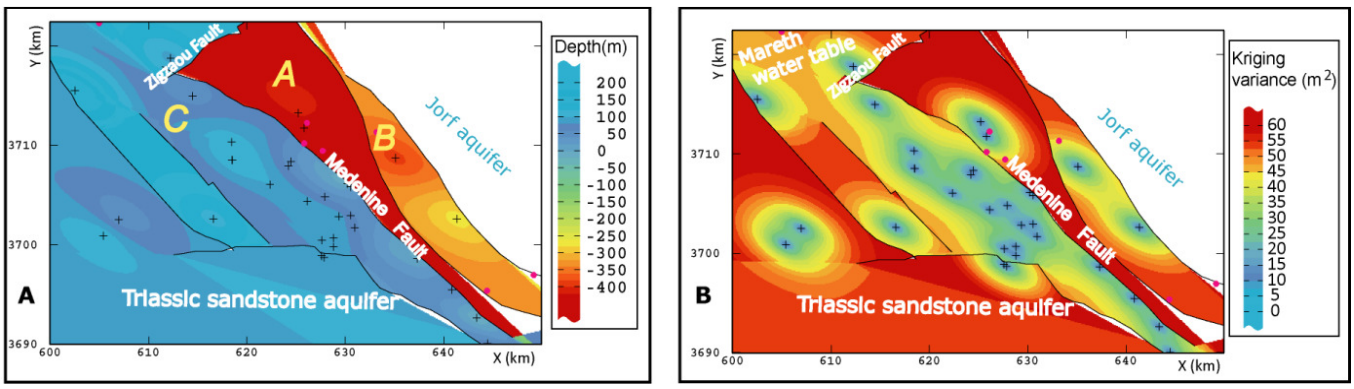

Fig. 11 A: Upper surface of the Turonian reservoir estimated by OK. (+: exact data, •: inequality data), C: central compartment, A and B NE downlifted compartments. B: Kriging variance map

DOI: 10.5963/JWRHE0503002

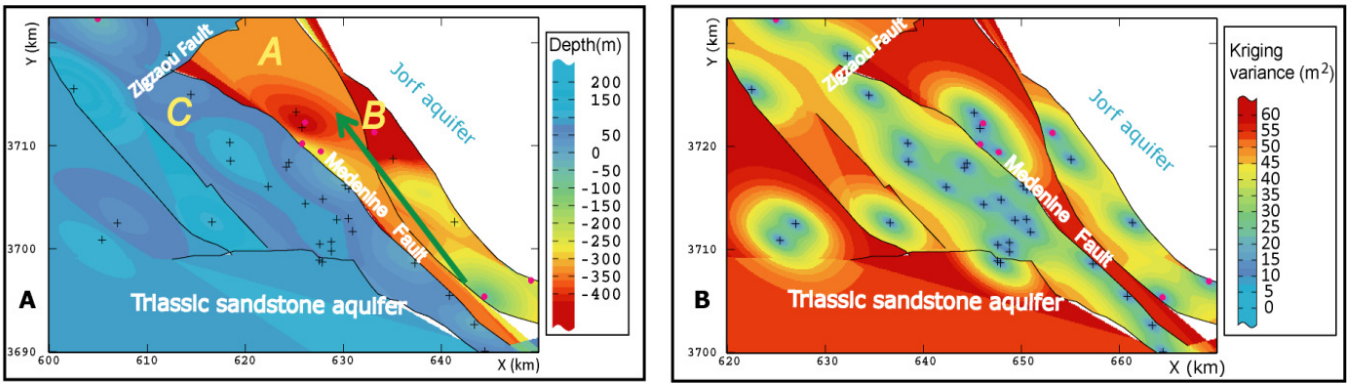

Fig. 12 A: Upper surface of the Turonian reservoir estimated by KI. (+: exact data, •: inequality data), C: central compartment, A and B NE downlifted compartments. B: Kriging variance map

4) Limitations and Improvements

The method of kriging with inequality presented some limitations at the beginning of its implementation in ISATIS software. Unfortunately, it was not possible to apply this approach in a domain where we have only inequality data, as shown on the kriged map of the Jurassic reservoir in the northeast downlifted compartment (Fig. 13A).

Interestingly enough, the method of kriging with inequality has been improved to overcome such limitations and implemented within the ISATIS Software. The method was then used to efficiently calculate the Jurassic Top, even in compartments where there are only inequality data (Fig. 13B).

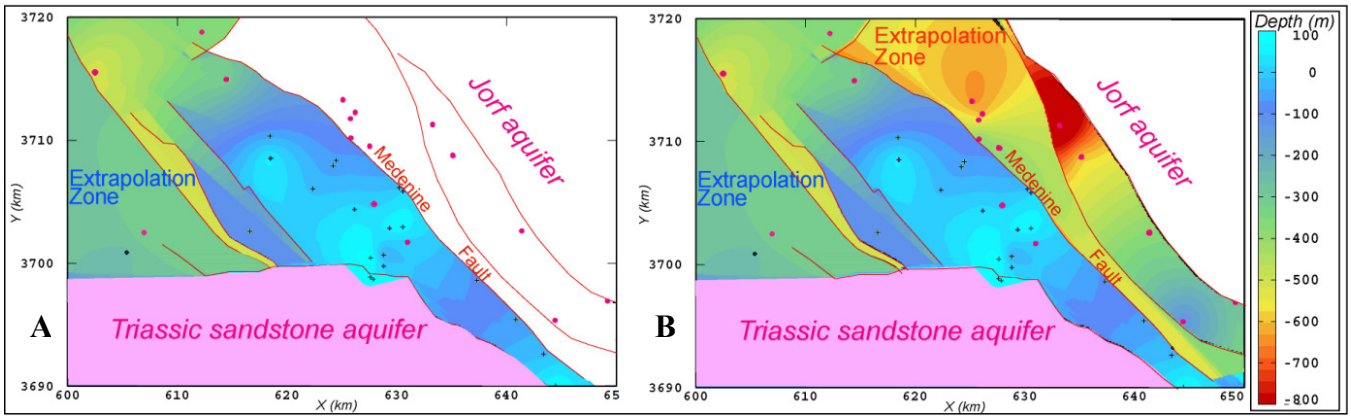

Fig. 13 Top Jurassic map estimated by KI before improvement (A) and after improvement (B)

(+: exact data, •: inequality data)

The improved KI method was also used to calculate the remaining bounding surfaces of the aquifer system units, included between the Jurassic and the Mio-Plio-Quaternary Tops. Fig. 14 shows the Top Cenomanian and the Top Senonian maps calculated by kriging with inequality.

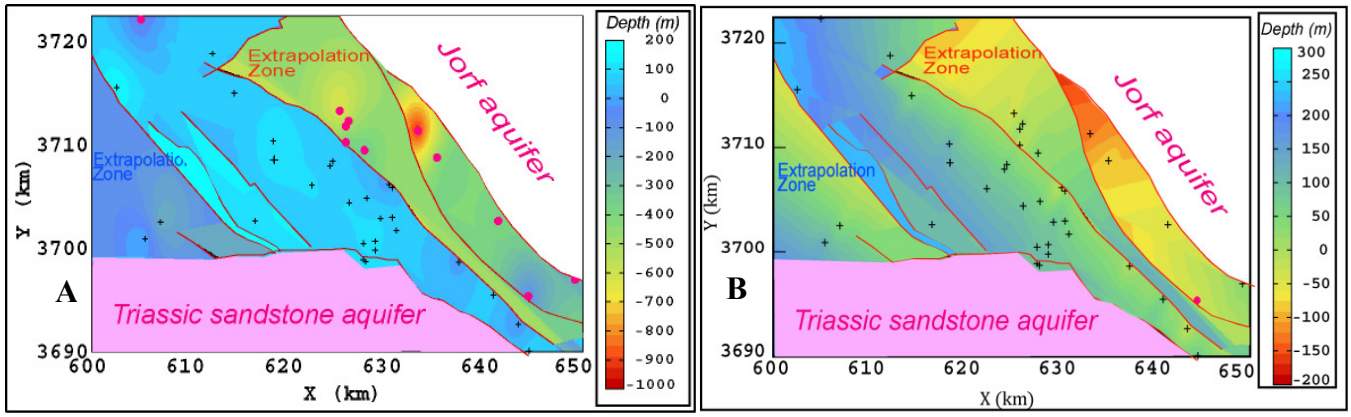

Fig. 14 Depth map of the Top Cenomanian (A) and Top Senonian (B) estimated by KI

(+: exact data, •: inequality data)

DOI: 10.5963/JWRHE0503002

IV. VALIDATION OF MODELLING RESULTS

The common first way of validating estimation results using kriging with inequality is via a kriging variance map. Fig. 15 displays the spatial distribution of uncertainties, as an example, of the Jurassic Horizon. It shows that the interpolations are reliable around the observations, even in areas including only inequality data. The kriging variance increases as the data density decreases at the borders of the compartments devoid of any data.

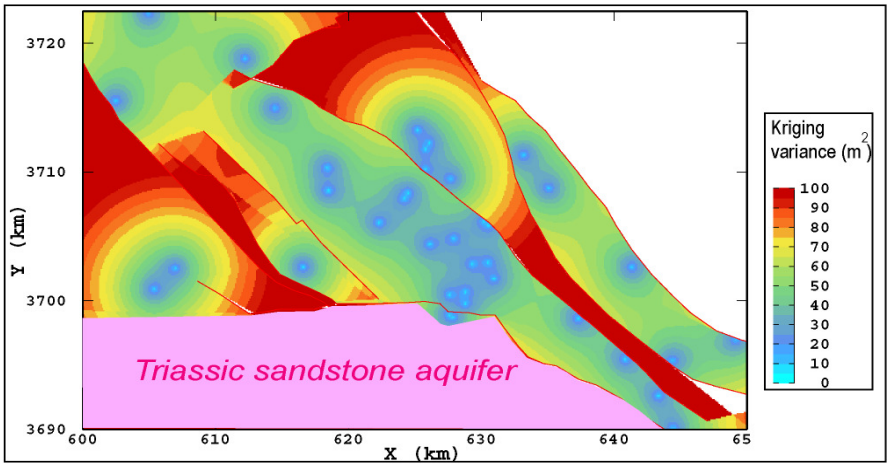

Fig. 15 Kriging variance map of the Jurassic Horizon

Fig. 16 shows the 3D visualizations of the bounding surfaces calculated by kriging with inequality.

Validating the estimation of the geological interfaces may be efficiently complemented by checking its consistency with the geological reality. Actually, the topology of the reconstructed surfaces should honor the observations deduced from the boreholes, that is, the stacking pattern generated by the geologist when interpreting the lithostratigraphic cross-sections.

A thorough trend analysis of the estimated geological interfaces leads to the following observations.

The depth map calculated by OK (Fig. 11A) reflects the compartmentalization and the overall downtilting to the northeast direction. However, the surface represents an important inconsistency within the northeast downlifted compartments; it displays a planar geometry in the northeast compartment (A) and a smooth topography in the northeast compartment (B). In fact, the data are scarce there, and do not allow reproduction of the surface geometry.

The depth map calculated by kriging with inequality (Fig. 12A) reflects the compartmentalization and the overall downtilting to the northeast direction. Moreover, the surface geometry honors the geological realism within the northeast downlifted compartment; it reproduces the downtilting of the surface to the northwest direction in compartments (A) and (B).

The downtilting within the northeast downlifted compartment is reproduced even for the surfaces where only inequality data are available, as is shown in Fig. 13B for the Jurassic Top and Fig. 14A for the Cenomanian Top.

DOI: 10.5963/JWRHE0503002

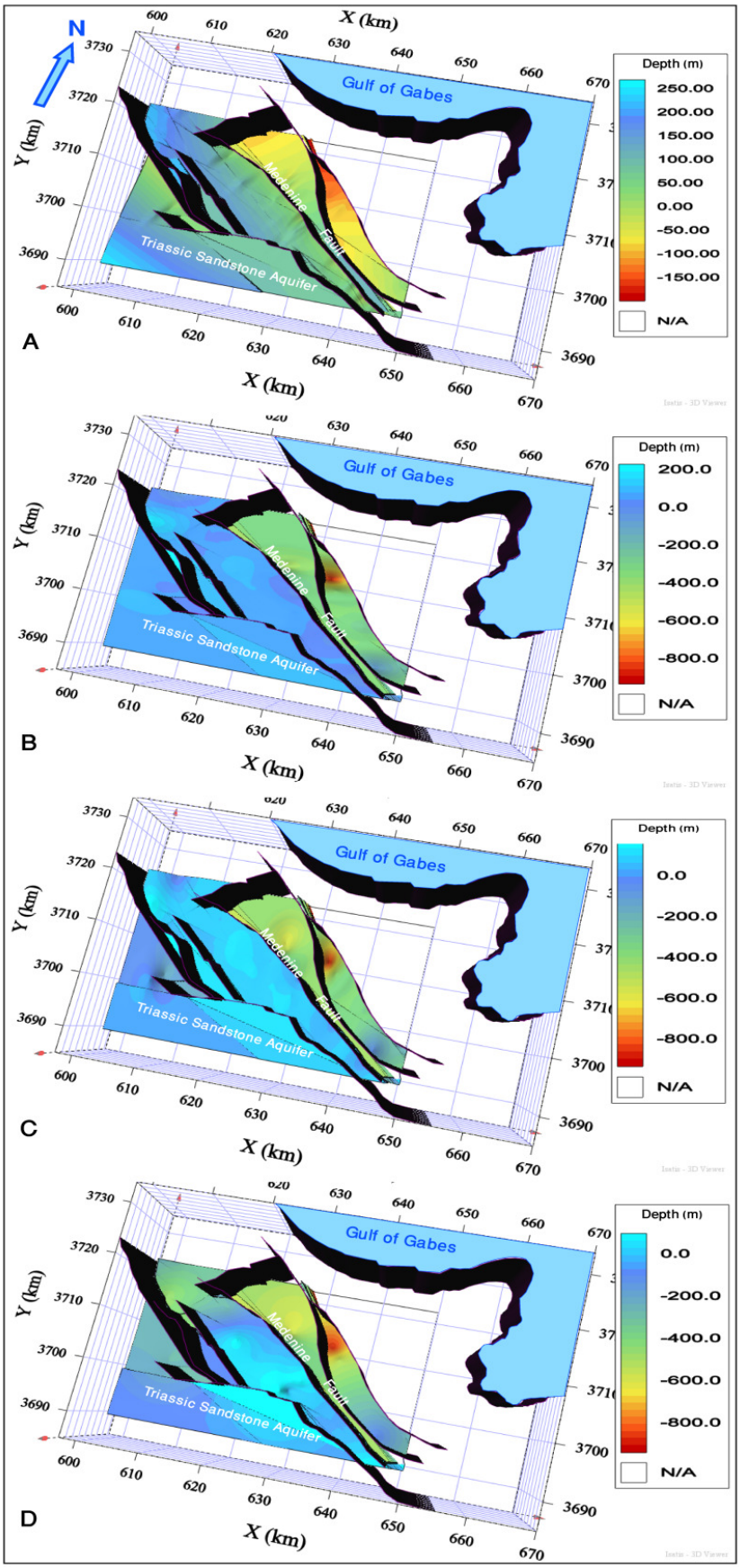

Fig. 16 3D Visualization of the Top Senonian (A), Top Turonian (B), Top Cenomanian (C) and Top Jurassic (D) maps calculated by kriging with inequality

DOI: 10.5963/JWRHE0503002

V. CONCLUSIONS

In this study, we aimed to build an architectural model of the "Jeffara de Medenine" aquifer system by modelling the faulted geological interfaces independently.

Different interpolation methods were attempted, such as reconstructing faulted surfaces to honor the data and reproduce the geological properties. Two main issues were addressed: *(i)* scarcity and uneven density of data, and *(ii)* the large variability of geometric parameters because of the faulting system.

A promising approach was developed, consisting of *(i)* dividing the aquifer into structural compartments, which allows respecting of the local variability, and *(ii)* taking into account the inequality information obtained from the bottom end of boreholes in order to increase the neighborhood size and the estimation accuracy within the considered compartment.

The combined use of KI and geological restrictions such as faults represents a promising direction for reliable structural mapping in the case of scarce data.

However, some areas, especially near the borders, are under-informed because the depth values are available only at very few wells. The approach did not give a reliable estimation and, thus, did not reproduce the geological reality.

The future outlook of the present study, to enhance the estimation of geological interfaces, consists of looking for an appropriate procedure to pursue extension of soft data from geological knowledge. This is necessary to overcome the gap between scarce measurements of geological and hydraulic parameters and modelling requirements. Therefore, this will make it possible to try more geostatistical methods and to integrate more adequate techniques for an accurate assessment.

ACKNOWLEDGMENT

This work was realized within the framework of the project "Geological modelling of the Jeffara aquifer systems, characterization of the *hydraulic* connectivity throughout *structural features*", which was financially supported by the Tunisian Ministry of Higher Education and Scientific Research. The authors would like to thank Tunisian National Oil Company and General Directorate for Water Resources for providing seismic, petroleum well and borehole data.

REFERENCES

[1] B. Ben Baccar, "Contribution à l'étude hydrogéologique de l'aquifère multicouche de Gabès Sud, " Doctoral thesis. University of Paris Sud, Orsay, France, 1982.

[2] A. Mammou, "Caractéristiques et évaluation des ressources en eau du Sud Tunisien," PhD thesis. University of Paris-Sud, Orsay, France, 1990.

[3] H. Yahyaoui, H. Chaieb, and M.Ouessar, "Impact des travaux de conservation des eaux et des sols sur la recharge de la nappe de Zeuss-Koutine," In: de Graff and Ouessar (Editors). Water *harvesting in Mediterranean zones: an impact assessment and economic evaluation. Proceedings from EU Wahia project final seminar in Lanzarote, Tropical Resources* Management Papers, 40, Wageningen University, The Netherlands, pp. 71–86, 2002.

[4] H. Chihi, G. de Marsily, H. Belayouiand, and H. Yahyaoui, "Relationship between tectonic structure and hydrogeochemical compartmentalization in aquifers: Example of the "Jeffara de Medenine" system, south-east Tunisia," *Journal of Hydrology: Regional Studies*, vol. 4 (2015), pp. 410–430. dx.doi.org/10.1016/j.ejrh, 2015.

[5] M. Ben Youssef and B. Peybernes, "Données micropaléontologiques et biostratigraphiques nouvelles sur le Crétacé inférieur marin du Sud-Tunisien," *J. African Earth Sci*., vol. l5, pp. 217–231, 1986.

[6] H. Ben Ouezdou, "Etude morphologique et stratigraphique des formations quaternaires dans les alentours du Golfe de Gabès," Doctoral thesis. Faculté des Sc. Humaines et Sociales, Tunis, Tunisia, 1983.

[7] G. Castany, "L'accident Sud-tunisien son âge et ses relations avec l'accident sud-atlasique d'Algérie," Note H. Devaux, *Bulletin de la Société Française de Physique*, 1954.

[8] P. F. Burollet, "Structures and tectonics of Tunisia," *Tectonophysics*, vol. 195, pp. 359–369, 1991.

[9] W. F. Bishop, "Geology of Tunisia and adjacent parts of Algeria and Libya," Association of Petroleum Geologists Bulletin, vol. 59(3), pp. 413–450, 1975.

[10] G. Busson, "Le Mésozoïque saharien 1ère partie: l'extrême-Sud tunisien," Publications du Centre de Recherches sur les Zones Arides (CNRS) Paris *série Géologie*, vol. 8, 194 p., 1967.

[11] S. Bodin, L. Petitpierrea, J. Wooda, I. Elkanouni and J. Redfern, "Timing of early to mid-cretaceous tectonic phases along North Africa: New insights from the Jeffara escarpment (Libya–Tunisia)," *J. of African Earth Sciences*, vol. 58(3), pp. 489–506, 2010.

[12] S. Bouaziz, E. Barrier, J. Angelier, P. Tricart and M. M. Turki, "Tectonic evolution of Southern Tethyan margin in southern Tunisia," In: S. Crasquin-Soleau and E. Barrier, Editors, *Peri-Tethys Memoir: 3. Stratigraphy and Evolution of Peri-Tethyan Platforms Mem. Mus. Natl. Hist. Nat.*, vol. 177, pp. 215–236, 1998.

[13] H. Chihi, B. Bedir and H. Belayouni, "Variogram Identification Aided by a Structural Framework for Improved Geometric Modelling of Faulted Reservoirs: Jeffara Basin, Southeastern Tunisia," *Natural Resources Research*, vol. 22(2), pp. 139–161, 2013. DOI: 10.1007/s11053-013-9201-0.

[14] H. Chihi, N. Jeannée, H. Yahyaoui, H. Belayouni and M. Bedir, "Geostatistical optimization of water reservoir characterization case of

DOI: 10.5963/JWRHE0503002

the "Jeffra de Medenine" aquifer system (SE Tunisia)," *Desalination and Water treatment*, vol. 2(10–12), pp. 2009–2016, 2014. DOI: 10.1080/19443994.2013.812988, 2014.

[15] Geovariances ISATIS, "Technical references," Fontainebleau, France, 2012.

[16] G. Matheron, "The theory of regionalized variable and its application," *Cah. Cent. Morphol. Math. Fontainebleau*5**,** France, 1971.

[17] A. G. Journel and Ch. J. Huijbregts, "Mining Geostatistics," Academic Press, pp. 26–95, 1978.

[18] G. Marsily de, "Quantitative Hydrogeology. Groundwater Hydrology for Engineers," Academic Press, New-York, 1986.

[19] M. Isaak and R. M. Srivastava, "An Introduction to Applied Geostatistics," Oxford University Press, New York, 1989.

[20] H. I. Edward and M. R. Srivastava, "Applied geostatistics," Oxford University Press, Oxford, 1989.

[21] J. P. Delhomme, "Application de la théorie des variables régionalisées dans les Sciences de l'eau," Eng. thesis. Université Paris VI, France, 1976.

[22] J. P. Chilès and D. Delfiner, "Geostatistics: Modelling Spatial Uncertainty," John Wiley & Son Interscience Publication, New-York, 2012.

[23] G. Marsily, F. de Delay, J. Goncalves, P. Renard V. Teles and S. Violette, "Dealing with spatial heterogeneity," *Hydrogeol Journal*, vol. 13, 2005.

[24] S. Ahmed, S. Sankaran and C.P. Gupta, "Variographic analysis of some hydrogeological parameters: use of geological soft data," *Journal of Environmental Hydrology*, vol. 3(2), 1995.

[25] P. Goovaerts, "Geostatistics for natural resources evaluation," Oxford University Press Oxford, 1997.

[26] H. Chihi and G. Marsily de, "Simulating Non-Stationary Seismic Facies Distribution in a Prograding Shelf Environment," *Oil & Gas Sciences and Technology*, vol. 64(4), pp. 451–467, 2009.

[27] H. Chihi, M. Tesson, A. GALLI, G. Marsily de and C. Ravenne, "Modélisation géostatistique (3D) des surfaces enveloppe d'unités stratigraphique à partir de profils sismiques: exemple de la partie médiane (Languedoc) de la plate-forme continentale du Golfe du Lion," *Bulletin de la société Géologique de France*, vol. 1, pp. 25–39, 2007.

[28] S. Gemanand and D. Geman, "Stochastic relaxation, Gibbs distribution and the Bayesian restoration of images," I.E.E.E. Trans. *Pattern Analysis and Machine Intelligence*, vol. 6, pp. 721–741, 1984.

[29] L. Bazzanna, P. Ruffo and D. Renard, " Estimation de cartes de profondeur conditionnées par des inégalités," *Cahier de Géostatistique* Ecole des Mines de Paris, France, pp. 23–43, 1995.

Hayet Chihi, Associated Professor at the Centre for Water Research and Technologies (CERTE), Tunisia, graduated as an engineer in geology from the Faculty of Sciences of Tunis (FST). She also has a Postgraduate Diploma in Geostatistics from Paris School of Mines, and a PhD thesis in Applied Geology and Geostatistics from University Paris VI jointly with the French Institute of Petroleum "IFP". She obtained an accreditation to supervise research (HDR) in 2014 from FST in Geostatistical Reservoir Characterization.

She started her professional experience at FST. She moved then to CERTE, and has been in charge of several collaborative research projects dealing with geostatistical modelling of geological objects. She has focused her activities in reservoir systems modelling constrained by geological properties and multi-source data. She has been teaching geostatistics for many years in several Tunisian engineering schools and faculties.

She is a member of IAMG and ATUGE.

H. Chihi, G. de Marsily, H. Belayoui and H. Yahyaoui, "Relationship between tectonic structure and hydrogeochemical compartmentalization in aquifers: Example of the "Jeffara de Medenine" system, south-east Tunisia". *Journal of Hydrology: Regional Studies*, vol. 4 (2015), pp. 410–430. dx.doi.org/10.1016/j.ejrh, 2015.

M. SOUA and H. Chihi "Optimizing exploration procedure using Oceanic anoxic events as a new tool for hydrocarbon strategy in Tunisia," In: Advances in Data, Methods, Models and Their Applications in Oil/Gas Exploration. Ed. Science Publishing Group, 65 pages, 2015.

H. Chihi and G. Marsily de, "Simulating Non-Stationary Seismic Facies Distribution in a Prograding Shelf Environment," *Oil & Gas Sciences and Technology*, vol. 64(4), pp. 451–467, 2009.

Ghislain de Marsily, emeritus Professor at Sorbonne Universities (Paris VI), France, is member of the French Academy of Sciences, Academy of Technologies, Foreign Associate of the US National Academy of Engineering, and member of the Academia Europaea. He graduated as a mining engineer and has taught Hydrology at the Paris School of Mines and Applied Geology at University Paris VI.

Within his scientific career, de Marsily has covered a wide range of research fields, including basin analysis, fluid mechanics, solute transport, waste disposal, river ecology, surface hydrology as well as hydrogeology, water resources management and worldwide food production, global water resources and sustainable development.

G. de Marsily "Stochastic description of flow in porous media," In: Encyclopedia of Physical Science and Technology, Yearbook 2001, Academic Press, San Diego, pp. 95-104, 2001.

G. de Marsily "Sols et ressources en eau," In: Les Sols, C. Feller, Ed. Belin et AFES, 2015.

G. de Marsily and R. Abarca Del Rio "Water and Food in the 21st Century," *Submitted to Surveys in Geophysics, Springer,* 2015.

DOI: 10.5963/JWRHE0503002

Matthieu Bourges graduated as an engineer in Geology (Master's degree) in 2007 from the Ecole Nationale Supérieure de Géologie (Nancy, France).

He is currently a geostatistician consultant (since 2007) at Geovariances (Avon, France). He is in charge of basic and advanced geostatistical trainings, consulting and mentoring. He has run more than 30 trainings in various countries in different fields of application of Geostatistics (for Oil & Gas and the environment, among others). He also contributes to Isatis (Geovariances) software support and pre-sales activities.

Mohamed Sbeaa graduated as a Geosciences engineer from the Faculty of Sciences of Tunis, University Tunis El Manar, in 2013. In his thesis project, he achieved a combined approach involving geophysical-petrophysical analysis for characterization and 3D modelling of the Ordovician paleovalleys in Ghdames Basin.

He is currently working as a research engineer at Centre for Water Research and Technologies, Tunisia. He is involved in the Jeffara Project, where he is in charge of geodatabase development and reservoir characterization in the “Jeffara de Gabes” area.

DOI: 10.5963/JWRHE0503002